Available online at www.sciencedirect.com
SCIENCE DIRECT
Geochimica et Cosmochimica Acta 70 (2006) 858–870
Geochimica
www.elsevier.com/locate/gca

The effect of crystallinity on dissolution rates and CO_2 consumption capacity of silicates

Domenik Wolff-Boenisch [a,b,*], Sigurdur R. Gislason [a], Eric H. Oelkers [c]

[a] *Institute of Earth Sciences, University of Iceland, Sturlugata 7, 101 Reykjavík, Iceland*
[b] *University of California, Merced, CA 95301, USA*
[c] *Géochimie et Biogéochimie Experimentale—LMTG/Université Paul Sabatier, 14 rue Edouard Belin, 31400 Toulouse, France*

Received 16 November 2004; accepted in revised form 25 October 2005

Abstract

Comparison of measured far-from-equilibrium dissolution rates of natural glasses and silicate minerals at 25 °C and pH 4 reveals the systematic effects of crystallinity and elemental composition on these rates. Rates for both minerals and glasses decrease with increasing Si:O ratio, but glass dissolution rates are faster than corresponding mineral rates. The difference between glass and mineral dissolution rates increases with increasing Si:O ratio; ultra-mafic glasses (Si:O $\leqslant 0.28$) dissolve at similar rates as correspondingly compositioned minerals, but Si-rich glasses such as rhyolite (Si:O ~ 0.40) dissolve $\geqslant 1.6$ orders of magnitude faster than corresponding minerals. This behaviour is interpreted to stem from the effect of Si–O polymerisation on silicate dissolution rates. The rate controlling step of dissolution for silicate minerals and glasses for which Si:O > 0.28 is the breaking of Si–O bonds. Owing to rapid quenching, natural glasses will exhibit less polymerisation and less ordering of Si–O bonds than minerals, making them less resistant to dissolution. Dissolution rates summarized in this study are used to determine the Ca release rates of natural rocks at far-from-equilibrium conditions, which in turn are used to estimate their CO_2 consumption capacity. Results indicate that Ca release rates for glasses are faster than those of corresponding rocks. This difference is, however, significantly less than the corresponding difference between glass and mineral bulk dissolution rates. This is due to the presence of Ca in relatively reactive minerals. In both cases, Ca release rates increase by ~two orders of magnitude from high to low Si:O ratios (e.g., from granite to gabbro or from rhyolitic to basaltic glass), illustrating the important role of Si-poor silicates in the long-term global CO_2 cycle.

1. Introduction

Natural glasses are less stable than igneous minerals at the Earth's surface because the glass retains more energy from its parent magma than the minerals (Gíslason and Arnórsson, 1990). Glassy rocks are rare, though not unknown, in Palaeozoic as compared to Tertiary formations. In contrast, glassy rocks 4×10^9 years old are found on the Moon. This observation lead Carmichael et al. (1974) to conclude that water migration rather than time alone is the controlling factor in devitrification (crystallisation) of terrestrial glasses. Although the weathering of both glassy and crystalline Ca,Mg-silicates plays a pivotal role in the long-term carbon dioxide cycle and soil formation in volcanic terrains (cf. Gaillardet et al., 1999; Kump et al., 2000; Chadwick and Chorover, 2001; Dessert et al., 2003), no study to date has provided a systematic comparison between dissolution rates of natural glasses and minerals as a function of their chemical composition. Several studies, however, have focussed on the effect of crystallinity on the dissolution rates of minerals and glasses having a single composition. For example, Gislason and Eugster (1987) observed that basaltic glass dissolved an order of magnitude faster than its crystalline analogue at pH 9–10. Hamilton et al. (2000) reported that the dissolution rate of albite was insignificantly different from that of synthetic albite

* Corresponding author. Fax: +1 209 724 4424.
E-mail address: dwolff-boenisch@ucmerced.edu (D. Wolff-Boenisch).

0016-7037/$ - see front matter © 2005 Elsevier Inc. All rights reserved.
doi:10.1016/j.gca.2005.10.016

glass. Stefánsson and Gíslason (2001) found that the chemical denudation rate of mobile elements in river catchments containing glassy basalts was 2–5 times faster than those comprised of fully crystalline basalts. The objective of the present study is to illustrate the effect of crystallinity on dissolution kinetics as a function of chemical composition and to use the results to estimate the relative CO_2 consumption capacity for a variety of natural rocks.

2. Theoretical background and data base development

Natural silicates are comprised of a variety of metal–oxide bonds and their dissolution requires the breaking of some or all of these bond types. Of the bonds present in these silicates, Si–O bonds tend to be the strongest and slowest to break during dissolution (Oelkers, 2001). It follows that the dissolution rates of natural silicates would be systematically related to the number of Si–O bonds present and the degree to which these Si–O bonds are bridged together to form a polymerized Si–O network. To assess this possibility, the Si:O ratio was chosen to illustrate the compositional variation of rates in the present study. This ratio has the advantage of (1) being readily calculated, (2) being representative of the relative number of Si–O bonds in the structure, and (3) providing a proxy for the degree of Si–O bond polymerisation; the higher the Si:O ratio, the more Si–O bonds are polymerized. For example, quartz has a Si:O ratio of 0.5 and all bonds in its structure are Si–O bonds. There are no non-bridging oxygens (NBO) within quartz and the structure is totally three-dimensionally polymerized. In contrast, forsterite has a Si–O ratio of 0.25 and $\leqslant$50% of the bonds in its structure are Si–O bonds. Owing to the large number of Mg cations in this structure, all Si–O tetrahedra are isolated and no Si–O polymerisation is present.

This study focuses on the variation of dissolution rates as a function of crystallinity. Crystallinity is treated in the present study as a categorical rather than a continuous variable. Although natural minerals and glasses studied in the laboratory may contain impurities, minerals are assumed to be 100% crystalline and glasses 100% amorphous. It seems reasonable to expect that crystallinity affects dissolution rates due to its effect on Si–O polymerisation. Si–O tetrahedra are the building blocks of silicate minerals and glasses. Within minerals, Si–O tetrahedra are attached to none, one, two, three or four other tetrahedra by bridging oxygens to form a regular, geometrically repeating pattern, over a large scale of unit cells (Doremus, 1994). In contrast, although glass contains silica tetrahedra, they do not exhibit the large scale regularity of minerals. Rapid quenching inhibits the ordered arrangement of the three-dimensional Si–O network beyond some adjacent unit cells. So the difference in polymerisation between a 'crystalline' mineral and an 'amorphous' glass lies in the degree of long-range order of silicate tetrahedra in the structure. Note, however, that crystallinity is not the only parameter that effects Si–O polymerisation, so too does chemical composition. For example, a 100% crystalline mineral like forsterite has no Si–O polymerisation whereas a 100% amorphous glass like obsidian exhibits a high degree of Si–O polymerisation due to its high SiO_2 content.

The importance of polymerisation and its relationship to the mineral's reactivity has been previously explored in the literature, although different parameters have been selected in an attempt to quantify this relationship. Brantley and Chen (1995) suggested that the logarithms of the dissolution rate constants of single-chain, double-chain, and isolated silicates correlate inversely with the number of bridging oxygens per Si–O tetrahedron, a term they called connectedness. This approach suggests the breaking of Si–O–Si bridging bonds as the rate limiting step of the dissolution reaction. Brantley (2003) reported a linear correlation between the logarithm of mineral dissolution rates and their ratio of non-tetrahedral to tetrahedral cations (X/Si). Others have reported linear correlations between the free energy of hydration ΔG_{hyd} and the logarithm of Si release rates for a wide array of chemically distinct glasses (Jantzen and Plodinec, 1984; Perret et al., 2003).

Dissolution rates are commonly considered to be proportional to the reactive surface area (cf. Helgeson et al., 1984; Hochella and Banfield, 1995). As this surface area is impossible to measure at present, dissolution rates are commonly normalized to either the experimentally measured BET specific surface area (A_{BET}) or the theoretically derived geometric specific surface area (A_{geo}) (cf. Brantley et al., 1999; Oelkers, 2002). A_{BET} is commonly significantly greater than A_{geo} because the former includes contributions of surface roughness, whereas the latter is computed assuming all grains have smooth geometric shapes. Dissolution rates normalized to A_{BET} are therefore substantially slower than those normalized to A_{geo}. The geometric specific surface area in the present study is calculated using

$$A_{geo} = \frac{6}{\rho \cdot d}, \tag{1}$$

where ρ designates the density of the solid and d refers to the average particle diameter. The number 6 is based on the assumption that grains have a regular spherical or cubic shape. Dissolution rates normalized to both A_{BET} and A_{geo} (r_{BET}, r_{geo}) are considered below to assess the variation of these rates as a function of composition and crystallinity.

Dissolution rates of silicate minerals, natural glasses, and synthetic glasses were compiled from the literature and are summarized in Table 1. Rates have been divided by the number of moles of Si per mole of the corresponding mineral or glass enabling clearer dissolution rate comparison. The only criteria for the selection of these dissolution rates were that they had been measured at or close to pH 4 and 25 °C. A pH of 4 was selected for this comparison rather than a circum-neutral pH, as acid conditions help avoid secondary phase precipitation and facilitate rate measurements at far-from-equilibrium conditions. Moreover, these conditions are close to that found in many

Table 1
Dissolution rates of silicate minerals and glasses at 25 °C and pH 4 taken from the literature

Reference	Mineral/glass	pH	Temp. (°C)	SA/V or flow rate[a] (cm^{-1} ml/min)	Density (g/cm^3)	Molar volume (cm^3/mol)	Size fraction (μm)	A_{BET} (cm^2/g)	A_{geo} (cm^2/g)	$\log(r_{BET}/n_{Si})$ ($mol_{Si}/m^2/s$)	$\log(r_{geo}/n_{Si})$ ($mol_{Si}/m^2/s$)	Lifetime (y)	Si:O
Chou and Wollast (1984)	Albite	3.5	22	0.15	2.62	100	50–100	750	317	−11.1	−10.8	54,723	0.38
Hellmann (1994)	Albite	4.0	25	0.1–3.0	2.62	100	—	130	—[c]	−11.1	−10.9	75,604	0.37
Knauss and Wolery (1986)	Albite	4.0	25	0.02	2.62	100	75–125	860	234	−11.9	−11.3	182,836	0.38
Welch and Ullman (1996)	Albite	4.0	22	4.0	2.62	102	125–250	530	127	−10.6	−10.0	8723	0.37
Swoboda-Colberg and Drever (1993)	Andesine, An30	4.0	25	0.08	2.66	100	75–150	—	208	—	−10.2	13,834	0.34
Oxburgh et al. (1994)	Andesine, An46	4.0	22	0.08	2.67	101	75–150	2000	208	−10.7	−9.8	4610	0.32
Stillings et al. (1996)	Andesine, An47	4.0	25	0.10	2.67	101	75–100	2000	259	−10.7	−9.9	5756	0.32
Welch and Ullman (1996)	*Andesine*, An49	4.0	22	4.0	2.68	101	125–250	770	124	−10.2	−9.4	1812	0.32
Welch and Ullman (1996)	*Andesine*, An49	4.0	22	4.0	2.68	101	125–250	710	124	−9.7	−9.0	750	0.32
Amrhein and Suarez (1992)	Anorthite, An93	4.3–4.6	25	**6**	2.73	102	20–50	5000	671	−10.8	−10.0	5820	0.26
Oelkers and Schott (1995)	Anorthite, An96	4.0	25	Open	2.73	102	50–100	414	305	−9.0	−8.9	484	0.25
Chen and Brantley (1998)	Anthophyllite	3.5	25	0.01	3.21	243	38–500	12,070	104	−12.4	−10.3	20,853	0.36
Siegel and Pfannkuch (1984)	Augite	4.0	22	**216**	3.40	71	38–42	11,000[b]	442	−11.2	−9.8	5662	0.33
Acker and Bricker (1992)	Biotite	4.0	22	0.17	3.20	140	149–420	8400	74	−11.1	−9.0	722	0.30
Kalinowski and Schweda (1996)	Biotite	4.0	22	0.07–0.33	3.09	295	10–20	55900	1346	−11.2	−9.6	2231	0.29
Malmström and Banwart (1997)	Biotite	4.0	25	0.05–0.25	3.09	144	75–125	18100	198	−11.6	−9.7	3389	0.32
Swoboda-Colberg and Drever (1993)	Biotite	4.0	25	0.08	3.09	140	75–150	—	179	—	−9.1	855	0.30
Oxburgh et al. (1994)	Bytownite, An76	4.0	22	0.08	2.71	101	75–150	2000	205	−10.0	−9.0	652	0.28
Welch and Ullman (1996)	Bytownite, An77	4.0	22	4.0	2.71	101	125–250	750	123	−9.1	−8.3	142	0.28
Brandt et al. (2003)	Chlorite	4.0	25	0.54	7.14	174	63–200	11,000	71	−11.5	−9.3	1807	0.27
Chen and Brantley (1998)	Diopside	3.5	25	0.01	3.40	64	75–150	1390	163	−10.9	−10.0	10,249	0.33
Knauss et al. (1993)	Diopside	4.1	25	0.02	3.40	64	75–125	550	180	−9.8	−9.3	2202	0.33
Schott et al. (1981)	Diopside	4.0	22	**5**	3.40	64	85–125	600	170	−9.1	−8.5	329	0.33
Oelkers and Schott (2001)	Enstatite	4.0	25	Open	3.20	63	50–100	800	260	−10.0	−9.5	1498	0.33
Schott et al. (1981)	Enstatite	4.0	22	**5**	3.25	63	85–125	5500	178	−11.1	−9.7	4436	0.33
Kalinowki et al. (1998)	Epidote	4.1	22	0.08-0.17	3.45	138	2–50	26,000	1607	−11.7	−10.4	18,979	0.29
Kalinowki et al. (1998)	Epidote	4.0	25	0.08-0.17	3.45	138	125–250	1275	96	−12.2	−11.1	80,517	0.29
Wogelius and Walther, 1992	Fayalite, Fo6	4.0	25	Open	4.39	46	250–420	307	42	−8.7	−7.8	42	0.25
Pokrovsky and Schott (2000)	Forsterite, Fo91	4.2	25	0.98	3.27	43	50–100	1600	254	−9.0	−8.2	126	0.25
Pokrovsky and Schott (2000)	Forsterite, Fo91	4.2	25	0.75	3.27	43	50–100	800	254	−8.7	−8.2	115	0.25
Wogelius and Walther (1991)	Forsterite, Fo91	4.0	25	Open	3.27	45	250–420	307	56	−9.1	−8.4	162	0.25
Rosso and Rimstidt (2000)	Forsterite, Fo92	3.8	25	1.15	3.27	45	250–350	356	62	−8.8	−8.1	82	0.25
Ragnarsdottir (1993)	Heulandite	4.0	25	0.03	2.20	326	75–125	1715	279	−10.8	−10.0	7733	0.32
Cygan et al. (1989)	Hornblende	4.0	25	**246.5**	3.23	268	37–149	49,300	231	−11.9	−9.6	3466	0.34
Frogner and Schweda (1998)	Hornblende	4.0	25	0.18	3.23	257	125–250	2800	103	−11.5	−10.1	11,579	0.34
Swoboda-Colberg and Drever (1993)	Hornblende	4.0	25	0.08	3.23	254	75–150	—	172	—	−10.2	14,870	0.32
Zhang et al. (1996)	Hornblende	4.0	25	**9.8**	3.23	268	110–250	980	109	−11.0	−10.0	8188	0.29
Zhang et al. (1996)	Hornblende	4.0	25	**8.6**	3.23	268	250–500	860	52	−11.0	−9.8	4350	0.29
Zhang and Bloom (1999)	Hornblende	4.2	25	**24.0**	3.23	268	250–500	2400	52	−11.7	−10.1	8767	0.29
Siegel and Pfannkuch (1984)	*Hypersthene*	4.0	22	**216**	3.60	66	38–42	11,000[b]	469	−11.7	−10.3	16,299	0.28
Köhler et al. (2003)	Illite	3.6	25	Closed	2.75	144	0.1–0.3	1,240,000	11,9849	−14.0	−13.0	7,578,570	0.36
Cama et al. (2002)	Kaolinite	4.0	25	0.01	2.60	99	<2	179,000	23,078	−13.7	−12.8	3,760,131	0.40
Carroll-Webb and Walther (1988)	Kaolinite	4.0	25	Batch	2.60	99	0.4–1	112,000	35,242	−12.9	−12.3	1,422,819	0.40
Ganor et al. (1995)	Kaolinite	4.0	25	0.02	2.60	99	0.5–2	100,000	21328	−12.0	−11.3	283,798	0.40
Huertas et al. (1999)	Kaolinite	3.8	25	163	2.60	99	<2	81,600	23,078	−14.1	−13.5	21,405,285	0.40
Wieland and Stumm (1992)	Kaolinite	4.0	25	**770**	2.60	99	0.5–2	154,000	21,328	−12.1	−11.3	116,220	0.40

Zysett and Schindler (1996)	K-montmorillonite	4.0	25	**37,450**	2.35	161	<2	—	25,618	—[d]	−12.2	1,368,142	0.40
Zysett and Schindler (1996)	K-montmorillonite	4.0	25	**37,450**	2.35	161	<2	—	25,618	—[d]	−12.0	813,344	0.40
Siegel and Pfannkuch (1984)	Labradorite, An53	4.0	22	**216**	2.70	102	38–42	11,000	557	−11.3	−10.0	7913	0.31
van Hees et al. (2002)	Labradorite, An59	3.5	25	0.08	2.70	101	90–125	1070	209	−10.3	−9.5	2659	0.30
Cygan et al. (1989)	Labradorite, An60	4.0	25	**9.5**	2.70	101	25–75	1900	489	−11.2	−10.6	28,566	0.30
Siegel and Pfannkuch (1984)	Microcline	4.0	22	**216**	2.56	106	38–42	11,000[b]	596	−11.8	−10.5	6442	0.38
Swoboda-Colberg and Drever (1993)	Microcline	4.0	25	0.08	2.56	109	75–150	—	217	—	−10.2	15,186	0.38
van Hees et al. (2002)	Microcline	3.5	25	0.08	2.56	106	125–250	1132	132	−11.4	−10.5	25,999	0.38
Kalinowski and Schweda (1996)	Muscovite	4.0	22	0.07–0.33	2.82	296	10–20	74,100	1475	−11.5	−9.8	4553	0.33
Swoboda-Colberg and Drever (1993)	Muscovite	4.0	25	0.08	2.82	141	75–150	—	197	—	−10.0	7075	0.30
Oxburgh et al. (1994)	Oligoclase, An13	4.0	22	0.08	2.65	100	75–150	2000	209	−11.5	−10.5	27,603	0.36
Swoboda-Colberg and Drever (1993)	Oligoclase, An16	4.0	25	0.08	2.65	100	75–150	—	209	—	−10.1	11,663	0.35
Cygan et al. (1989)	Oligoclase, An24	4.0	25	**36.5**	2.65	100	37–149	7300	282	−12.3	−10.9	75,330	0.35
Siegel and Pfannkuch (1984)	Olivine, Fo83	4.0	22	**216**	3.32	46	38–42	13,000	452	−11.3	−9.8	4766	0.25
Kalinowski and Schweda (1996)	Phlogopite	4.0	22	0.07–0.33	2.80	298	10–20	55,900	1485	−11.3	−9.7	3307	0.28
Bennett (1991)	Quartz	3.0	25	**50**	2.62	23	30–75	1700	466	−13.2	−12.6	6,013,754	0.50
Brady and Walther (1990)	Quartz	4.0	25	**64**	2.62	23	74–149	1110	214	−12.2	−11.5	452,286	0.50
Gíslason et al. (1997)	Quartz	3.5	25	Open	2.62	23	74–250	485	158	−14.6	−14.1	164,040,536	0.50
Welch and Ullman (1996)	Quartz	4.0	22	4.0	2.62	23	125–250	510	127	−10.9	−10.3	24,600	0.50
Amram and Ganor (2005)	Smectite	4.1	25	0.01	2.35	318	<2	—	25,618	—[d]	−13.2	13,202,779	0.39
Amram and Ganor (2005)	Smectite	4.0	25	0.02	2.35	318	<2	—	25,618	—[d]	−12.7	4,014,844	0.39
Casey et al. (1993)	Tephroite	4.2	25	Batch	4.25	48	25–75	1100	310	−6.1	−5.5	0.2	0.25
Rimstidt and Dove (1986)	Wollastonite	3.9	23.5	15.8	2.84	41	150–250	5460	108	−7.9	−6.2	1.3	0.33
Rimstidt and Dove (1986)	Wollastonite	4.0	23.5	15.8	2.84	41	150–250	1600	108	−7.3	−6.1	1.0	0.33
Rimstidt and Dove (1986)	Wollastonite	3.9	23.5	15.8	2.84	41	150–250	7000	108	−7.7	−5.9	0.6	0.33
Weissbart and Rimstidt (2000)	Wollastonite	4.1	25	6.17	2.84	41	150–250	3020	117	−8.6	−7.2	11	0.33
Weissbart and Rimstidt (2000)	Wollastonite	3.9	25	12.93	2.84	41	150–250	3020	117	−8.6	−7.2	12	0.33
Hamilton et al. (2001)	g-Albite	4.0	25	1–2	2.38	110	74–149	705	235	−11.0	−10.5	28,670	0.37
Gislason and Oelkers (2003)	g-Basalt	4.2	30	4.08	3.05	110	40–120	23,000	270	−10.3	−8.4	72	0.30
Guy and Schott (1989)	g-Basalt	4.0	25	Closed	2.95	123	135–200	—	123	—	−9.1	847	0.30
Hamilton et al. (2001)	g-Jadeite	4.0	25	1–2	2.43	83	74–149	644	230	−10.6	−10.2	10,784	0.33
Hamilton et al. (2001)	g-Nepheline	4.0	25	1–2	2.50	57	74–149	891	224	−9.5	−8.9	444	0.25
White (1983)	g-Perlite	4.0	25	25	2.36	124	211–423	2300	83	−11.1	−9.7	3838	0.41
Mazer and Walter (1994)	g-Silica	4.1	25	**0.3–0.6**	2.20	27	—	—	38-69	—	−12.2	1,768,712	0.50
Plettinck et al. (1994)	g-Silica	4.0	25	**63**	2.20	27	1–63	25,000	1822	−12.4	−11.3	215,947	0.50
Wolff-Boenisch et al. (2004a)	BT, rhyolite	4.2	25	0.96	2.31	113	45–125	31,210	332	−11.5	−9.5	3271	0.41
Wolff-Boenisch et al. (2004a)	Ö62, rhyolite	4.1	25	1.04	2.36	112	45–125	4300	324	−11.0	−9.9	6419	0.40
Wolff-Boenisch et al. (2004a)	H1, rhyolite	4.0	25	1.09	2.42	109	45–125	5590	317	−11.0	−9.8	5538	0.40
Wolff-Boenisch et al. (2004a)	H3W, rhyolite	4.1	25	1.00	2.42	109	45–125	10,760	316	−11.0	−9.5	2975	0.40
Wolff-Boenisch et al. (2004a)	A75, rhyolite	4.1	25	1.09	2.45	108	45–125	14,090	312	−11.3	−9.6	3716	0.39
Wolff-Boenisch et al. (2004a)	H3B, dacite	4.0	25	1.06	2.51	107	45–125	12,100	305	−10.7	−9.1	1220	0.38
Wolff-Boenisch et al. (2004a)	HZ0, dacite	4.0	25	0.97	2.59	105	45–125	6240	296	−10.9	−9.5	2972	0.36
Wolff-Boenisch et al. (2004a)	SLN, dacite	4.1	25	0.96	2.55	107	45–125	26470	301	−11.2	−9.3	1670	0.37
Wolff-Boenisch et al. (2004a)	H20, andesite	4.1	25	1.14	2.79	102	45–125	1185	275	−10.1	−9.4	2103	0.33
Wolff-Boenisch et al. (2004a)	HZ1, andesite	4.0	25	0.92	2.73	104	45–125	21,550	280	−10.9	−9.0	816	0.32
Wolff-Boenisch et al. (2004a)	GR, basalt	4.1	25	0.90	2.99	97	45–125	1120	256	−9.8	−9.2	1167	0.31
Wolff-Boenisch et al. (2004a)	HEI, mugearite	4.2	25	0.95	2.81	103	45–125	710	272	−9.4	−9.0	750	0.31
Wolff-Boenisch et al. (2004a)	A61, basalt	4.1	25	0.93	2.99	98	45–125	1445	256	−9.9	−9.1	1028	0.31
Wolff-Boenisch et al. (2004a)	KRA, basalt	4.1	25	0.95	3.04	97	45–125	1400	252	−9.8	−9.0	884	0.31

(*continued on next page*)

Table 1 (*continued*)

Reference	Mineral/glass	pH	Temp. (°C)	SA/V or flow rate[a] (cm^{-1} ml/min)	Density (g/cm^3)	Molar volume (cm^3/mol)	Size fraction (μm)	A_{BET} (cm^2/g)	A_{geo} (cm^2/g)	$\log(r_{BET}/n_{Si})$ ($mol_{Si}/m^2/s$)	$\log(r_{geo}/n_{Si})$ ($mol_{Si}/m^2/s$)	Lifetime (y)	Si:O
Wolff-Boenisch et al. (2004a)	KAT, basalt	4.2	25	0.96	3.04	97	45–125	9400	252	−10.4	−8.8	489	0.30
Wolff-Boenisch et al. (2004a)	SS, basalt	4.2	25	0.92	3.00	98	45–125	1945	255	−9.8	−9.0	655	0.29
Wolff-Boenisch et al. (2004a)	ELD, basalt	4.0	25	0.92	3.02	98	45–125	52,240	253	−11.2	−8.9	552	0.29

Also provided in this table are the Si:O ratio, density, specific surface area of each solid as well as some aspects of the experimental technique used to measure rates.

[a] Entries that appear in bold face denote surface area to volume ratios (SA/V), whereas entries in normal font represent flow rates. Mineral names in italic font were renamed according to their mineral composition and vary from the names given in the reference.

[b] The same as for labradorite according to the authors.

[c] The author estimates A_{BET} to be 1.5 times higher than A_{geo}.

[d] The authors determined mass normalized release rates.

Earth surface environments such as soils. In cases where rates had been determined at temperatures other than 25 °C, they were extrapolated to 25 °C with the temperature dependence provided by the corresponding authors. Note that rates listed in Table 1 were measured using a variety of open and closed system reactors; surface area to volume ratio of experiments performed in closed system reactors and the fluid flow rates of experiments performed in open systems are provided in this table. Rates determined in the presence of organic ligands, which may catalyse dissolution rates (Oelkers and Schott, 1998; Welch and Ullman, 1996) have not been included in Table 1. Similarly, dissolution rates reported in the literature that did not provide the chemical composition, size fraction and/or A_{BET} of the dissolving solids have also been omitted.

There are several inconsistencies in the database listed in Table 1. One of the most striking inconsistencies are the reported dissolution rates of kaolinite, where r_{BET} range from 10^{-14} mol/m^2/s reported by Huertas et al. (1999) to 10^{-12} mol/m^2/s reported by Ganor et al. (1995). There are several possible sources for these inconsistencies. First, the dissolution rates of numerous multi-oxide silicate minerals have been found to be strong functions of aqueous solution composition, even at far-from-equilibrium conditions (cf. Oelkers, 1996). For example, constant pH, far-from-equilibrium kaolinite dissolution rates at acid conditions have been found to be inversely proportional to the aqueous aluminium activity in the reactive solution (Oelkers et al., 1994; Devidal et al., 1997). Such solution composition effects tend to lower dissolution rates with time in batch reactors (Oelkers et al., 2001). Note the effect of solution composition on rates persists to extremely dilute solutions; e.g., the aqueous Al^{3+} activity has been found to affect pH 4 glass dissolution rates at Al^{3+} concentrations down to as low as 10^{-11} mol/kg (Wolff-Boenisch et al., 2004b). In addition, clay mineral dissolution rates have been reported to decrease with time in open system flow reactors (Köhler et al., 2005). The authors attributed this effect to a changing morphology of clay mineral grains during their progressive dissolution. These observations could account for the differences between the relatively low kaolinite dissolution rates measured in long-term batch experiments (Huertas et al., 1999) versus the relatively fast rates measured in shorter-term and/or open system experiments (Wieland and Stumm, 1992; Ganor et al., 1995). The effect of such inconsistencies on the comparison between silicate glass and mineral dissolution rates will be considered in more detail below.

3. Results and discussion

3.1. Rates as a function of composition and crystallinity

Logarithms of r_{BET} and r_{geo} of silicate minerals and glasses are listed in Table 1 and depicted by symbols as a function of the molar Si:O ratio of the solids in Figs. 1A and B. The solid and dashed lines in Fig. 1 represent linear

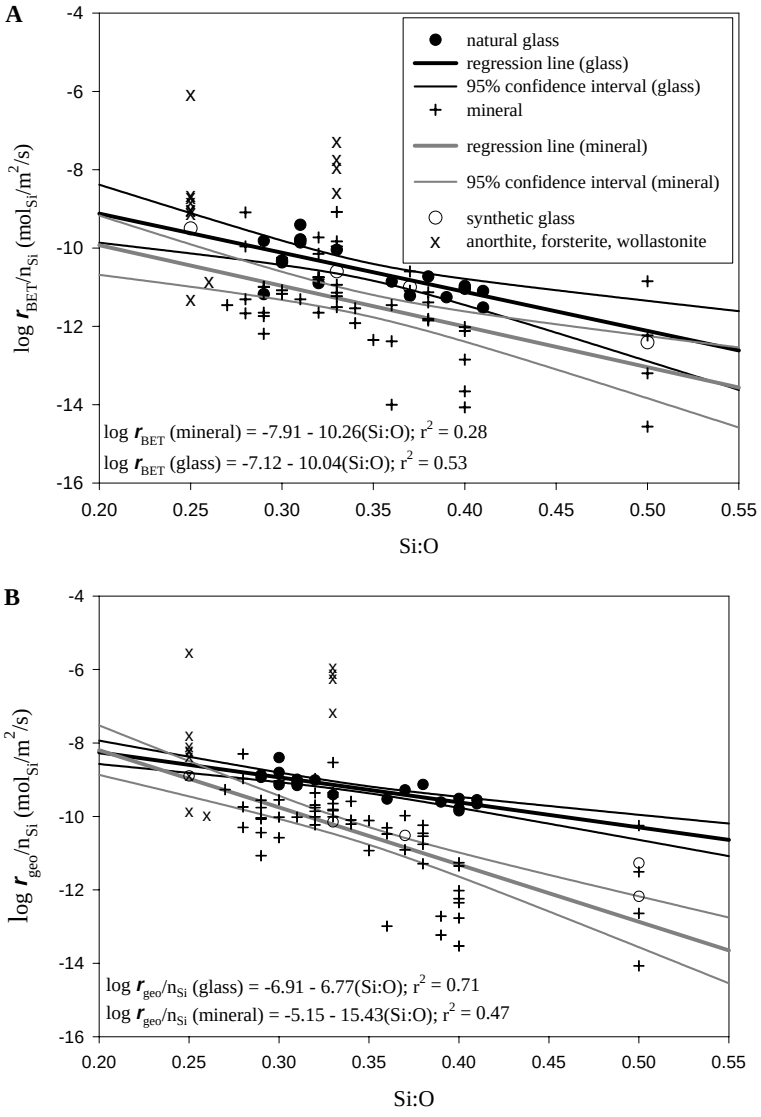

Fig. 1. The logarithm of dissolution rates of glasses and minerals divided by n_{Si} at pH 4 and 25 °C versus the molar ratio of silicon to oxygen in the structure (Si:O). (A) Dissolution rates normalized to BET surface area, whereas (B) displays rates normalized to geometric surface area. All rates are listed in Table 1 and plotted as symbols in both figures. The bold and thin black curves represent a linear least squares fit and associated 95% confidence intervals of the glass data, whereas the bold and thin grey curves represent a linear least squares fit and associated 95% confidence intervals of the mineral data. The dissolution rates of the minerals anorthite, forsterite, and wollastonite that were not included in the fit reflect the rates of breaking bonds other than Si–O as described in text.

least square fits of the data and the corresponding 95% confidence intervals of the fits, respectively. Three minerals were omitted when calculating the linear regression fits and correlation coefficients (r^2) in Figs. 1 and 2. The minerals forsterite and anorthite, which have Si:O ratios of 0.25, have so many octahedral cation–oxygen bonds in their structure that Si–O bonds need not be broken to dissolve these minerals. As a consequence their dissolution rates reflect the rate of breaking bonds other than Si–O, such as Mg–O bonds for the case of forsterite and Al–O bonds for the case of anorthite (cf. Oelkers, 2001). Dissolution rates of wollastonite (Si:O ratio 0.33) have been omitted because its dissolution at acid conditions leads to the rapid and complete removal of Ca from its surface causing extensive Ca-free leached layers (Casey et al., 1993; Weissbart and Rimstidt, 2000). Following formation of these leached layers, isolated Si–O chains are liberated at rates far faster than their lesser leached counterparts. Due to the fact that the dissolution rates of anorthite, forsterite, and wollastonite do not reflect the rate of breaking Si–O bonds present in the mineral structure they have been discarded from the regression calculations, but have been plotted in the figures.

It can be seen in Fig. 1A that r_{BET} generally decrease with increasing Si:O ratio. Minerals and glasses of similar Si:O ratios exhibit comparable dissolution rates, irrespective of their structure and crystallinity. The trendlines drawn in this figure correspond to

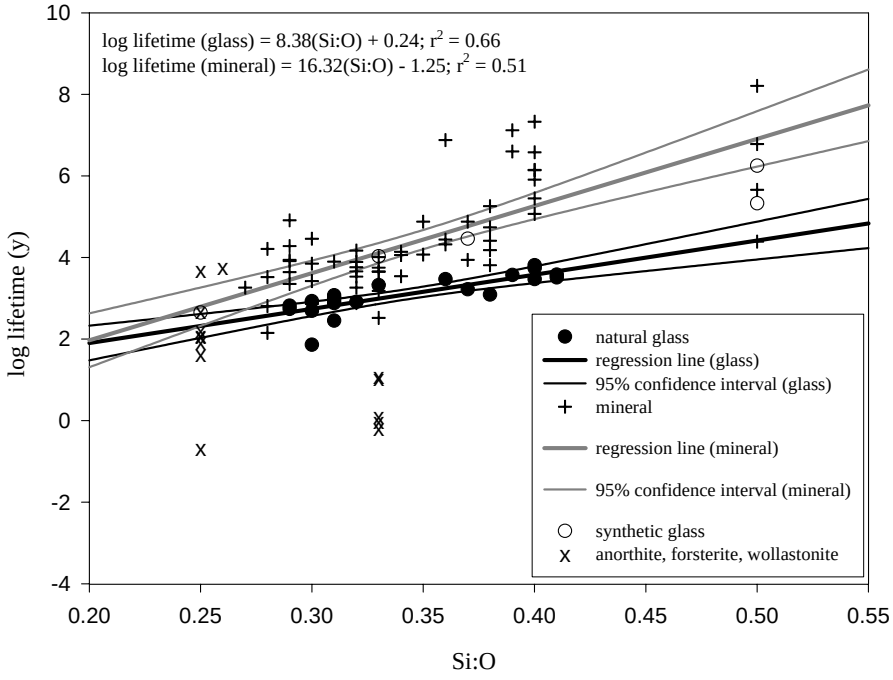

Fig. 2. The logarithm of lifetimes of 1 mm radius grains of minerals and glasses at 25 °C and pH 4 in far-from-equilibrium aqueous solutions as a function of their Si:O ratio. The lifetimes were computed using Eq. (4) together with rates listed in Table 1. The bold and thin black curves represent a linear least squares fit and associated 95% confidence intervals of the glass lifetimes, whereas the bold and thin grey curves represent a linear least squares fit and associated 95% confidence intervals of the mineral lifetimes.

$$\log(r_{BET}/n_{Si})\ \text{glass}\ (\text{mol/m}^2/\text{s}) = -7.12\text{–}10.04(\text{Si}:\text{O});\quad r^2 = 0.53 \tag{2a}$$

and

$$\log(r_{BET}/n_{Si})\ \text{mineral}\ (\text{mol/m}^2/\text{s}) = -7.91\text{–}10.26(\text{Si}:\text{O});\quad r^2 = 0.28 \tag{2b}$$

for natural glasses and minerals, respectively. n_{Si} in Eqs. (2a) and (2b) stands for the number of moles of Si in one mole of the corresponding mineral or glass, and r^2 represents the correlation coefficient. Both regression fits display similar slopes and the 95% confidence intervals for these fits overlap extensively, indicating that all data can be approximated with a single regression line. Similarly, linear least squares fits of the distribution of the logarithm of r_{geo} for natural glasses and silicate minerals as a function of their Si:O ratio were obtained and are presented in Fig. 1B. Equations describing these trends are given by

$$\log(r_{geo}/n_{Si})\ \text{glass}\ (\text{mol/m}^2/\text{s}) = -6.91\text{–}6.77(\text{Si}:\text{O});\quad r^2 = 0.71 \tag{3a}$$

and

$$\log(r_{geo}/n_{Si})\ \text{mineral}\ (\text{mol/m}^2/\text{s}) = -5.15\text{–}15.43(\text{Si}:\text{O});\quad r^2 = 0.47. \tag{3b}$$

Similar to their BET surface area normalized counterparts, r_{geo} decreases with increasing Si:O ratio for both natural glasses and silicate minerals. However, the absolute value of the slope of the linear correlation for silicate minerals is 2.3 times greater than that for natural glasses. As such r_{geo} for Si poor silicate minerals are comparable in value to those of glasses of similar Si:O ratios, but close to 2 orders of magnitude less than those of Si-rich glasses. Most significantly, r_{geo} provides a far better correlation with the Si:O ratio than does r_{BET}. The correlation coefficient (r^2) for the logr_{geo} versus Si:O ratio plots are 0.71 and 0.47, respectively, for glasses and minerals, whereas corresponding r^2 for log r_{BET} versus Si:O ratio plots are 0.53 and 0.28.

The observation that r_{geo} provides a more consistent description of the variation with composition of natural glass and silicate mineral dissolution rates than r_{BET} stems from the differences between A_{geo} and A_{BET}. A_{geo} is computed assuming surfaces are smooth geometric shapes and therefore A_{geo} does not vary significantly during most dissolution experiments. In contrast, A_{BET} includes contributions from a number of sources that may be relatively unreactive, including internal porosity and surface coatings (Jeschke and Dreybrodt, 2002; Hodson, 2003). A_{BET} has also been observed to vary significantly during laboratory dissolution experiments. For example, Stillings and Brantley (1995) reported that BET surface areas of feldspars increased by a factor of 2–10 during dissolution experiments performed at 25 °C. Gautier et al. (2001) found a fourfold increase in quartz BET surface area during dissolution experiments performed at 200 °C. A detailed discussion of the relative merits of normalizing dissolution rates to

A_{BET} versus A_{geo} is provided by Wolff-Boenisch et al. (2004a) for natural glasses and by Brantley (2003) for minerals.

It can be seen in Fig. 1B that the dissolution rates of synthetic silicate glasses are intermediate to those of silicate minerals and natural glasses. This observation may be related to the annealing rate used to create the synthetic glasses. For example, Hamilton et al. (2001) measured the dissolution rates of synthetic albite, jadeite, and nepheline glass which had been created via a slow annealing process. Such efforts may create glasses with far more ordered structures than rapidly annealed natural glasses.

Despite scatter, the general trends evident in Fig. 1B indicate that crystalline silicates with high Si:O ratios (Si:O $\geqslant$ 0.39) dissolve at least 1.6 orders of magnitude slower than their non-crystalline counterparts. This difference systematically diminishes with decreasing Si:O ratio until corresponding rates of silicate minerals and glasses are similar in magnitude. This happens at an Si:O ratio $\leqslant$0.28, where the 95% confidence intervals for minerals overlaps that of the glasses. It appears that the decrease of the difference between mineral and glass dissolution rates with decreasing Si:O ratio originates from the corresponding effect of crystallinity on the degree of Si:O polymerisation. As the breaking of Si:O bonds is the rate controlling step of dissolution for silicate minerals and glasses for which Si:O > 0.28, the degree of polymerisation of these bonds is critical for resisting dissolution. Owing to rapid quenching, natural glasses will exhibit less polymerisation and less ordering of Si–O bonds than minerals. The disorder in glass structures apparently destabilizes to a greater extent the Si–O polymerisation of Si-rich solids versus Si-poor solids. It is interesting to note that the 0.28 Si:O ratio below which silicate minerals and glasses appear to have similar dissolution rates, also corresponds to the Si:O ratio below which silicate minerals no longer have bridging Si–O–Si bonds.

3.2. The average lifetime of mineral and glass grains

The rates listed in Table 1 and illustrated in Fig. 1B enable estimation of the lifetimes of silicate minerals and glasses at far-from-equilibrium conditions. The time $\boldsymbol{t}$ required to completely dissolve a spherical grain is given by (Lasaga, 1998)

$$\boldsymbol{t} = \left(\frac{\boldsymbol{rad}}{\boldsymbol{V}_m \boldsymbol{r}_{geo}}\right), \tag{4}$$

where $\boldsymbol{rad}$ stands for the grain radius and $\boldsymbol{V}_m$ refers to the molar volume of the corresponding mineral or glass. The lifetimes of 1 mm radius spherical mineral and glass grains in highly undersaturated solutions were computed using Eq. (4) together with rates given in Table 1 and are illustrated as a function of Si:O ratio in Fig. 2. A linear correlation between grain lifetime and Si:O ratio was found and is provided in this figure. A 1 mm radius forsterite grain has a lifetime of ~120 years at pH 4 and 25 °C. Mineral grain lifetime increases exponentially with increasing Si content; a 1 mm radius quartz grain has a lifetime of 10^8 years. Similar to the relative distribution of glass versus mineral dissolution rates, Si-rich glasses are calculated to persist for ~2 orders of magnitude less time than their mineral counterparts. In contrast, Si-poor glasses are estimated to persist for approximately as long as their mineral counterparts.

3.3. Relative CO_2 fixation rates of glassy and crystalline rocks as a function of composition

Although the exact connection between laboratory measured and field rates is still being debated (e.g., White and Brantley, 2003) rates compiled in the present study enable estimation of the relative CO_2 fixation rates by weathering reactions. CO_2 fixation through this process has received considerable attention in the literature. For instance, the effect of sea floor weathering of submarine basalts (MORBs) on CO_2 fixation has been studied by François and Walker (1992), Spivack and Staudigel (1994), Caldeira (1995), Brady and Gislason (1997), and Alt and Teagle (1999). Similarly, Taylor and Lasaga (1999) and Dessert et al. (2001) suggested that the formation of large *continental* igneous provinces, such as the flood basalts of Columbia River and the Deccan Traps, provide a significant sink for atmospheric CO_2 via rapid dissolution of basaltic rocks. The relative CO_2 drawdown rates in the present study are estimated from the far-from-equilibrium Ca release rates of various rocks. The total release rate of Ca ($\boldsymbol{r}_{Ca}$) from a multi-mineral rock can be estimated using

$$\boldsymbol{r}_{Ca} = \sum_i (X_{Ca,i} * \boldsymbol{r}_{geo,i} * X_{Vol,i}), \tag{5}$$

where $X_{Ca,i}$ symbolizes the mole fraction of Ca in the ith mineral, $\boldsymbol{r}_{geo,i}$ represents the far-from-equilibrium geometric surface area normalized dissolution rate of the ith mineral, and $X_{Vol,i}$ stands for the volume fraction of the ith mineral in the rock. Note that Eq. (5) is based on the assumption that the relative surface areas of the minerals in a rock will be proportional to their volume fraction. The release rate of Ca is taken to be representative of the long-term CO_2 fixation rate because the bulk of Ca released by silicate weathering reactions is consumed by carbonate precipitation (Berner and Berner, 1996). The long term net effect is 1 mol of CO_2 fixed for each mole of Ca released from silicate weathering. $\boldsymbol{r}_{Ca}$ for a variety of silicate rocks and glasses have been determined from Eq. (5) together with mineral volume fractions listed in Table 2, and the $\boldsymbol{r}_{geo,i}$ of Ca bearing minerals and glasses listed in Table 1. The results of this calculation are illustrated in Fig. 3A. Note that $\boldsymbol{r}_{Ca}$ for rocks depend to a certain degree on the modal mineral composition of each rock; rocks of different compositions will have $\boldsymbol{r}_{Ca}$ that differ somewhat from those listed in Table 2.

Table 2
Estimated volume fractions of major minerals in common plutonic and volcanic rocks[a]

	QZ	KFSP	PL[b]	MICA	AMPH	CPX	OPX	OL	$\log r_{Ca}$	$\log r_{Mg}$	$\log r_{Ca+Mg}$	$\log r_{K+Na}$	$\log r_{Ca+Mg+K+Na}$	Si:O
Granite	0.25	0.4	0.26/An13	0.05	0.01	—	—	—	−12.3	−10.6	−10.6	−10.7	−10.3	0.40
Granodiorite	0.21	0.15	0.46/An30	0.03	0.13		—	—	−11.3	−10.8	−10.6	−10.7	−10.4	0.37
Diorite	0.02	0.03	0.64/An46	0.05	0.12	0.08	0.03	—	−10.6	−10.5	−10.2	−10.4	−10.0	0.33
Gabbro	—	—	0.65/An59	0.01	0.03	0.14	0.06	0.07	−10.3	−9.6	−9.5	−10.4	−9.4	0.30
Rhyolite/Granite[c]	0.3	0.4	0.2/An13	0.05	0.05	—	—	—	−11.9	−10.6	−10.6	−10.7	−10.3	0.40
Dacite/Granodiorite	0.1	0.1	0.5/An30	—	0.3		—	—	−11.1	−11.3	−10.9	−11.0	−10.6	0.37
Andesite/Diorite	—	—	0.65/An46	—	0.25	0.1	—	—	−10.5	−11.1	−10.4	−10.6	−10.2	0.33
Basalt/Gabbro	—	—	0.4/An76	—	—	0.25	0.05	0.3	−9.8	−8.9	−8.9	−10.3	−8.9	0.30

The compositions listed in this table were taken from McBirney (1992) and Best and Christiansen (2000). The logarithms of the elemental release rates computed using Eq. (3) or derived from it are also provided in this table, and units of r_{Ca}, r_{Mg}, r_{Ca+Mg}, r_{K+Na}, and $r_{Ca+Mg+K+Na}$ are (mol of the subscripted element or sum of elements released/m^2/s).

[a] The abbreviations QZ, KFSP, PL, MICA, AMPH, CPX, OPX, and OL refer to quartz, potassium feldspar, plagioclase, mica, amphibole, clino-pyroxene, ortho-pyroxene, and olivine, respectively.

[b] In addition to its volume fraction, the typical composition of the plagioclase is provided; the number after An refers to the anorthite percentage of the plagioclase.

[c] There is no difference between corresponding calculated plutonic/volcanic rock release rates because they are based on the dissolution of *minerals* whose dissolution rates are the same for any rock type.

Fig. 3A provides a simple relation for estimating the relative Ca release rates of natural glasses and rocks at far-from-equilibrium conditions during surface weathering. r_{Ca} for crystalline rocks are lower than those of natural glasses. This difference is, however, less than the corresponding difference between glass and mineral dissolution rates (cf. Fig. 1B). This result stems from the fact that Ca tends to be located in the more reactive silicate minerals of any given rock. According to the equations in Fig. 3A, basaltic glass releases Ca 2.8 times faster than gabbro (Si:O = 0.30), and rhyolitic glass releases Ca 4.9 times faster than granite (Si:O = 0.40). This effect of crystallinity on Ca release rates is similar to that found from river catchment studies reported by Stefánsson and Gíslason (2001).

Ca release rates, and therefore atmospheric CO_2 fixation rates are strong functions of the Si:O ratio of the rock. Ca release rates of a basalt or a gabbro (Si:O = 0.30), calculated using the linear regression in Fig. 3A, are two orders of magnitude faster than that of a rhyolite or granite (Si:O = 0.40), respectively. This effect of Si:O ratio on rates is significantly greater than the corresponding impact on dissolution rates shown in Fig. 1B because glasses and minerals of low Si:O ratio dissolve fast and are Ca rich, while minerals and glasses of high Si:O ratio dissolve slowly and are Ca poor.

Several studies have suggested that either the sum of Ca and Mg release rates or the sum of Ca, Mg, K, and Na release rates also provide good proxies for long- and short-term atmospheric CO_2 fixation, respectively, due to chemical weathering (Gislason et al., 1996; Gaillardet et al., 1999; Taylor et al., 1999; Dessert et al., 2003). Values of the sum of Mg and Ca release rates (r_{Ca+Mg}) and the sum of Ca, Mg, K, and Na release rates ($r_{Ca+Mg+Na+K}$) were computed by summing together release rates determined by an analogy of Eq. (5) together with rock compositions listed in Table 2. The results of these calculations are listed in Table 2 and illustrated in Figs. 3B and C. The most striking difference between r_{Ca}, r_{Ca+Mg}, and $r_{Ca+Mg+Na+K}$ is that the latter two show little effect of crystallinity. As is the case for calcium discussed above, magnesium is predominantly present in the more rapidly dissolving minerals, which compensates for the relatively fast dissolution rates of the glasses. The Si:O dependence of Ca and base cation release rates illustrated in Fig. 3 is greater than that deduced from river catchment studies (Meybeck, 1987; Bluth and Kump, 1994; Gibbs and Kump, 1994; Taylor et al., 1999). For example, Meybeck (1987) suggested that the gabbro weathering rate is only 1.3 times greater than that of granite. Taylor et al. (1999) concluded that the base cation release and CO_2 consumption rate of basalt is 3 times faster than that of granite. There are several possible reasons for this apparent discrepancy of the effect of rock chemical composition on metal release rates determined from the laboratory and field. The laboratory studies focus only on the dissolution contribution to the overall weathering process while field studies consider both dissolution and secondary mineral formation. Metal release rates computed in the present study are based on experiments performed in organic-free solutions at far-from-equilibrium conditions. In contrast, natural solutions may contain dissolved organic compounds which tend to accelerate the dissolution rates of the relatively slow dissolving alkali-feldspars far more than they accelerate the rates of rapidly dissolving olivines, pyroxenes, and Ca-feldspar (Welch and Ullman, 1996; Oelkers and Schott, 1998; Blake and Walter, 1999; Golubev et al., 2005). Equally, as basalt dissolves 10–100 times faster than rhyolite at far-from-equilibrium solutions, the solution can more readily approach equilibrium with either the minerals comprising basalt or with secondary minerals, such as smectites and zeolites, that can hinder elemental release from basalt.

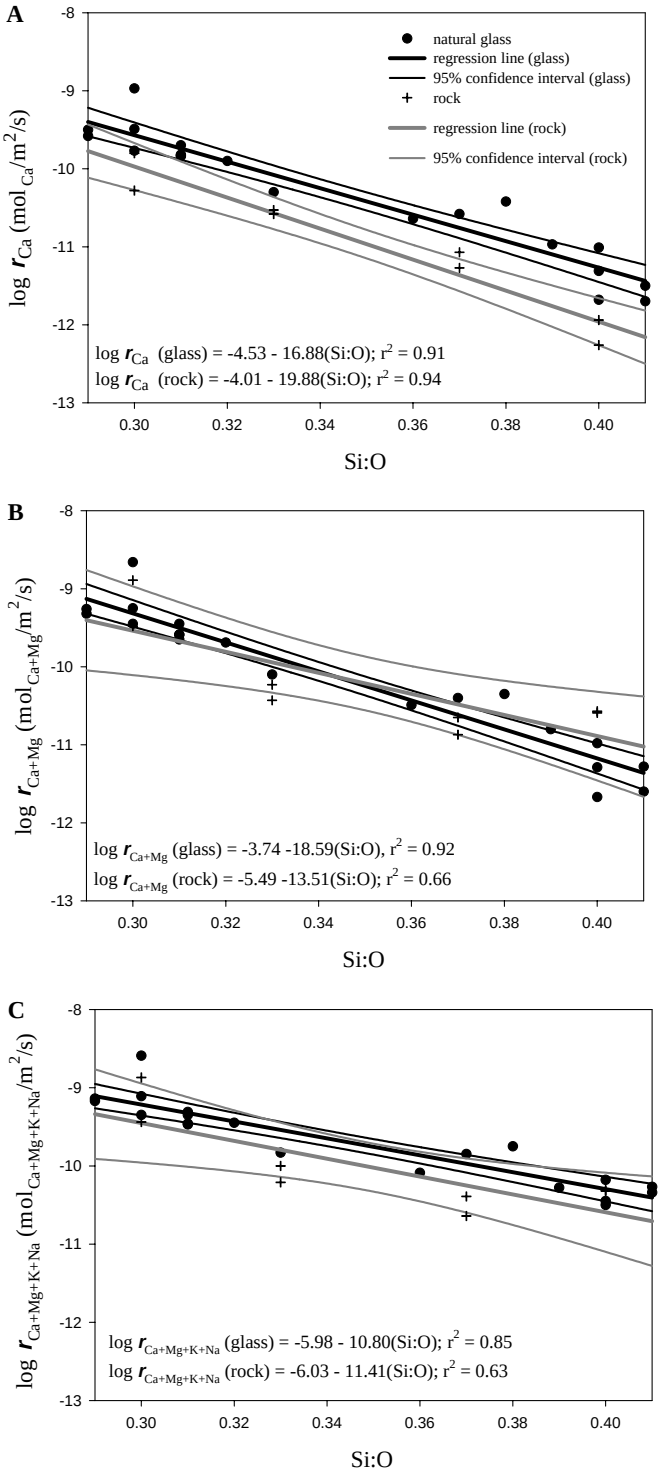

Fig. 3. Far-from-equilibrium elemental release rates of natural glasses and rocks at 25 °C and pH 4 versus their Si:O ratio. Release rates were determined using Eq. (5) and by calculating analogously elemental release rates for Mg, K, and Na. The composition of the rocks and details of this calculation are presented in Table 2. The bold and thin black curves represent a linear least squares fit and associated 95% confidence intervals of the glass data, whereas the bold and thin grey curves represent a linear least squares fit and associated 95% confidence intervals of the mineral data.

This suggests that basalt dissolution is more runoff dependent than rhyolite. Considering both, the relative abundance of granitic versus basaltic rocks and the relative inertness of granites versus basalts, it seems likely that granitic rock weathering has a relatively small effect on long-term atmospheric CO_2 evolution.

4. Conclusions

The results presented above illustrate the significance of crystallinity and composition on the dissolution rates of rock forming silicates. The major conclusions of this study are:

(1) Natural silicate glass dissolution rates are significantly faster than their crystalline counterparts only when they are Si-rich. Si-poor glasses and minerals (e.g., of ultrabasic composition) exhibit similar dissolution rates as crystallinity has little effect on Si polymerisation in these solids.
(2) The relative long-term CO_2 consumption capacity, as estimated through Ca release rates of natural silicate rocks is affected by the rocks' crystallinity, but less so than their overall dissolution rates. This is because Ca is commonly contained in relatively rapidly dissolving minerals in crystalline rocks.
(3) The relative long-term CO_2 consumption capacity, as estimated through Ca release rates of basaltic rocks is computed to be 2 orders of magnitude faster than that of granites and rhyolites. The relative inertness of silica-rich rocks relative to basalts suggests that the weathering of granites and rhyolites play only a minor role in long-term atmospheric CO_2 evolution.

Acknowledgments

We express our gratitude to Marijo Murillo, Malla Kristiansen, and Stacey Callahan for their ongoing personal support during the course of this study. This manuscript greatly benefited from reviews by the associate editor Liane Benning, Sue Brantley, and two anonymous reviewers. The study has been financed by the European Union through a Research Training Network titled "Dissolution and precipitation of solid solutions in natural and industrial processes" within the 5th framework programme (contract number: HPRN-CT-2000-00058) and the Institute of Earth Sciences, University of Iceland.

Associate editor: Liane G. Benning

References

Acker, J.G., Bricker, O.P., 1992. The influence of pH on biotite dissolution and alteration kinetics at low temperature. *Geochim. Cosmochim. Acta* **56**, 3073–3092.

Alt, J.C., Teagle, D.A.H., 1999. The uptake of carbon during alteration of ocean crust. *Geochim. Cosmochim. Acta* **63**, 1527–1535.

Amram, K., Ganor, J., 2005. The combined effect of pH and temperature on smectite dissolution rate under acidic conditions. *Geochim. Cosmochim. Acta* **69**, 2535–2546.

Amrhein, C., Suarez, D.L., 1992. Some factors affecting the dissolution kinetics of anorthite at 25 °C. *Geochim. Cosmochim. Acta* **56**, 1815–1826.

Bennett, P.C., 1991. Quartz dissolution in organic-rich aqueous systems. *Geochim. Cosmochim. Acta* **55**, 1781–1797.

Berner, E.K., Berner, R.A., 1996. *Global Environment, Water, Air, and Geochemical Cycles*. Prentice Hall, Englewood Cliffs, NJ.

Best, M.G., Christiansen, E.H., 2000. *Igneous Petrology*. Blackwell Science, Oxford.

Blake, R.E., Walter, L.M., 1999. Kinetics of feldspar and quartz dissolution at 70–80 °C and near-neutral pH: effects of organic acids and NaCl. *Geochim. Cosmochim. Acta* **63**, 2043–2059.

Bluth, G.J.S., Kump, L.R., 1994. Lithology and climatologic controls of river chemistry. *Geochim. Cosmochim. Acta* **58**, 2341–2359.

Brady, P.V., Walther, J.V., 1990. Kinetics of quartz dissolution at low temperatures. *Chem. Geol.* **82**, 253–264.

Brady, P.V., Gislason, S.R., 1997. Seafloor weathering controls on atmospheric CO_2 and global climate. *Geochim. Cosmochim. Acta* **61**, 965–973.

Brandt, F., Bosbach, D., Krawczyk-Bärsch, E., Arnold, T., Bernhard, G., 2003. Chlorite dissolution in the acid ph-range: a combined microscopic and macroscopic approach. *Geochim. Cosmochim. Acta* **67**, 1451–1461.

Brantley, S., 2003. Reaction kinetics of primary rock-forming minerals under ambient conditions. In: Drever, J. (Ed.), *Treatise on Geochemistry, Surface and Groundwater, Weathering and Soils*, vol. 5. Elsevier, Amsterdam, pp. 73–118.

Brantley, S.L., Chen, Y., 1995. Chemical weathering rates of pyroxenes and amphiboles. In: White, A.F., Brantley, S.L. (Eds.), Chemical Weathering Rates of Silicate Minerals. *Reviews in Mineralogy*, vol. 31, pp. 119–172.

Brantley, S.L., White, A.F., Hodson, M.E., 1999. Surface area of primary silicate minerals. In: Jamtveit, B., Meakin, P. (Eds.), *Growth, Dissolution and Pattern Formation in Geosystems*. Kluwer Academic Publishers, Rotterdam, pp. 291–326.

Caldeira, K., 1995. Long-term control of atmospheric carbon dioxide, Low-temperature seafloor alteration or terrestrial silicate rock weathering?. *Am. J. Sci.* **295** 1077–1114.

Cama, J., Metz, V., Ganor, J., 2002. The effect of pH and temperature on kaolinite dissolution rate under acidic conditions. *Geochim. Cosmochim. Acta* **66**, 3913–3926.

Carmichael, I.S.E., Turner, F.J., Verhoogen, J., 1974. *Igneous Petrology*. MacGraw-Hill, New York.

Carroll-Webb, S.A., Walther, J.V., 1988. A surface complex reaction model for the pH-dependence of corundum and kaolinite dissolution rates. *Geochim. Cosmochim. Acta* **52**, 2604–2623.

Casey, W.H., Westrich, H.R., Banfield, J.F., Ferruzzi, G., Arnold, G.W., 1993. Leaching and reconstruction at the surfaces of dissolving chain silicate minerals. *Nature* **366**, 253–255.

Chadwick, O.A., Chorover, J., 2001. The Chemistry of Pedogenic Thresholds. *Geoderma* **100**, 321–353.

Chen, Y., Brantley, S.L., 1998. Diopside and anthophyllite dissolution at 25 °C and 90 °C and acid pH. *Chem. Geol.* **147**, 233–248.

Chou, L., Wollast, R., 1984. Study of the weathering of albite at room temperature and pressure with a fluidized bed reactor. *Geochim. Cosmochim. Acta* **48**, 2205–2217.

Cygan, R.T., Casey, W.H., Boslough, M.B., Westrich, H.R., Carr, M.J., Holdren Jr., G.R., 1989. Dissolution kinetics of experimentally shocked silicate minerals. *Chem. Geol.* **78**, 229–244.

Dessert, C., Dupré, B., François, L.M., Schott, J., Gaillardet, J., Chakrapani, G.J., Bajpai, S., 2001. Erosion of Deccan Traps determined by river geochemistry: impact on the global climate and the $^{87}Sr/^{86}Sr$ ratio of seawater. *Earth Planet. Sci. Lett.* **188**, 459–474.

Dessert, C., Dupré, B., Gaillardet, J., François, L.M., Allègre, C.J., 2003. Basalt weathering laws and the impact of basalt weathering on the global carbon cycle. *Chem. Geol.* **202**, 257–273.

Devidal, J.L., Schott, J., Dandurand, J.L., 1997. An experimental study of kaolinite dissolution and precipitation kinetics as a function of chemical affinity and solution composition at 150 °C, 40 bars, and pH 2, 6.8, and 7.8. *Geochim. Cosmochim. Acta* **61**, 5165–5186.

Doremus, R.H., 1994. *Glass Science*. Wiley, New York.

François, L.M., Walker, J.C.G., 1992. Modelling the phanerozoic carbon cycle and climate. constraints from the $^{87}Sr/^{86}Sr$ isotopic ratio of seawater. *Am. J. Sci.* **292**, 81–135.

Frogner, P., Schweda, P., 1998. Hornblende dissolution kinetics at 25 °C. *Chem. Geol.* **151**, 169–179.

Gaillardet, J., Dupré, B., Louvat, P., Allègre, C.J., 1999. Global silicate weathering and CO_2 consumption rates deduced from the chemistry of the large rivers. *Chem. Geol.* **159**, 3–30.

Ganor, J., Mogollón, J.L., Lasaga, A.C., 1995. The effect of pH on kaolinite dissolution rates and on activation energy. *Geochim. Cosmochim. Acta* **59**, 1037–1052.

Gautier, J.-M., Oelkers, E.H., Schott, J., 2001. Are quartz dissolution rates proportional to BET surface areas? *Geochim. Cosmochim. Acta* **65**, 1059–1070.

Gibbs, M.T., Kump, L.R., 1994. Global chemical erosion during the last glacial maximum and the present: sensitivity to changes in lithology and hydrology. *Palaeoceanography* **9**, 529–543.

Gislason, S.R., Eugster, H.P., 1987. Meteoric water–basalt interactions. I. A laboratory study. *Geochim. Cosmochim. Acta* **51**, 2827–2840.

Gíslason, S.R., Arnórsson, S., 1990. Saturation state of natural waters in Iceland relative to primary and secondary minerals in basalts. In: Spencer, R.J., Chou, I.-M. (Eds.), *Fluid-Mineral Interactions. A Tribute to H.P. Eugster*, vol. 2. Geochemical Society, Special Publication, pp. 373–393.

Gislason, S.R., Arnórsson, S., Ármannsson, H., 1996. Chemical weathering of basalt in SW Iceland. Effects of runoff, age of rocks and vegetative/glacial cover. *Am. J. Sci.* **296**, 837–907.

Gíslason, S.R., Heaney, P.J., Oelkers, E.H., Schott, J., 1997. Kinetic and thermodynamic properties of moganite, a novel silica polymorph. *Geochim. Cosmochim. Acta* **61**, 193–1204.

Gislason, S.R., Oelkers, E.H., 2003. The mechanism, rates, and consequences of basaltic glass dissolution. II. An experimental study of the dissolution rates of basaltic glass as a function of pH at temperatures from 6 °C to 150 °C. *Geochim. Cosmochim. Acta* **67**, 3817–3832.

Golubev, S.V., Pokrovsky, O.S., Schott, J., 2005. Effect of dissolved CO_2 on the dissolution kinetics of basaltic silicates at 25 °C. *Chem. Geol.* **217**, 227–238.

Guy, C., Schott, J., 1989. Multisite surface reaction versus transport control during hydrolysis of a complex oxide. *Chem. Geol.* **78**, 181–204.

Hamilton, J.P., Pantano, C.G., Brantley, S.L., 2000. Dissolution of albite glass and crystal. *Geochim. Cosmochim. Acta* **64**, 2603–2615.

Hamilton, J.P., Brantley, S.L., Pantano, C.G., Criscenti, L.J., Kubicki, J.D., 2001. Dissolution of nepheline, jadeite and albite glasses. Toward better models for aluminosilicate dissolution. *Geochim. Cosmochim. Acta* **65**, 3683–3702.

Hellmann, R., 1994. The albite–water system. Part I. The kinetics of dissolution as a function of pH at 100, 200, and 300 °C. *Geochim. Cosmochim. Acta* **58**, 595–611.

Helgeson, H.C., Murphy, W.M., Aagaard, P., 1984. Thermodynamic and kinetic constraints on reaction rates among minerals and aqueous solutions. II. Rate constants, effective surface area, and the hydrolysis of feldspar. *Geochim. Cosmochim. Acta* **48**, 2405–2432.

Hochella, M.F., Banfield, J.F., 1995. Chemical weathering of silicates in nature: a microscopic perspective with theoretical considerations. *Rev. Min.* **31**, 353–406.

Hodson, M.E., 2003. The influence of Fe-rich coatings on the dissolution of anorthite at pH 2.6. *Geochim. Cosmochim. Acta* **67**, 3355–3363.

Huertas, F.J., Chou, L., Wollast, R., 1999. Mechanism of kaolinite dissolution at room temperature and pressure. Part II. Kinetic study. *Geochim. Cosmochim. Acta* **63**, 3261–3275.

Jantzen, C.M., Plodinec, M.J., 1984. Thermodynamic model of natural, medieval and nuclear waste glass durability. *J. Non-Cryst. Solids* **67**, 207–223.

Jeschke, A.A., Dreybrodt, W., 2002. Dissolution rates of minerals and their relation to surface morphology. *Geochim. Cosmochim. Acta* **66**, 3055–3062.

Kalinowski, B.E., Schweda, P., 1996. Kinetics of muscovite, phlogopite, and biotite dissolution and alteration at pH 1–4, room temperature. *Geochim. Cosmochim. Acta* **60**, 367–385.

Kalinowki, B.E., Faith-Ell, C., Schweda, P., 1998. Dissolution kinetics and alteration of epidote in acidic solutions at 25 °C. *Chem. Geol.* **151**, 181–197.

Knauss, K.G., Wolery, T.J., 1986. Dependence of albite dissolution kinetics on pH and time at 25 °C and 70 °C. *Geochim. Cosmochim. Acta* **50**, 2481–2497.

Knauss, K.G., Nguyen, S.N., Weed, H.C., 1993. Diopside dissolution kinetics as a function of pH, CO_2, temperature, and time. *Geochim. Cosmochim. Acta* **57**, 285–294.

Köhler, S.J., Dufaud, F., Oelkers, E.H., 2003. An experimental study of illite dissolution kinetics as a function of pH and temperatures from 5 to 50 °C. *Geochim. Cosmochim. Acta* **67**, 3583–3594.

Köhler, S.J., Bosbach, D., Oelkers, E.H., 2005. Do clay mineral dissolution rates reach steady-state? *Geochim. Cosmochim. Acta* **69**, 1997–2006.

Kump, L.R., Brantley, S.L., Arthur, M.A., 2000. Chemical weathering, atmospheric CO_2, and climate. *Annual Rev. Earth Planet. Sci.* **28**, 611–667.

Lasaga, A.C., 1998. *Kinetic Theory in Earth Sciences*. Princeton University Press, New Jersey.

Mazer, J.J., Walter, J.V., 1994. Dissolution kinetics of silica as a function of pH between 40 and 85 °C. *J. Non-Cryst. Solids* **170**, 32–45.

Malmström, M., Banwart, S., 1997. Biotite dissolution at 25 °C: the pH dependence of dissolution rate and stoichiometry. *Geochim. Cosmochim. Acta* **61**, 2779–2799.

McBirney, A.R., 1992. *Igneous Petrology*, second ed. Jones and Bartlett Publishers, Boston.

Meybeck, M., 1987. Global chemical weathering of surficial rocks estimated from river dissolved loads. *Am. J. Sci.* **287**, 401–428.

Oelkers, E.H., 1996. Summary and review of the physical and chemical properties of rocks and fluids. *Rev. Min.* **34**, 131–191.

Oelkers, E.H., 2001. A general kinetic description of multi-oxide silicate mineral and glass dissolution. *Geochim. Cosmochim. Acta* **65**, 3703–3719.

Oelkers, E.H., 2002. The surface area of rocks and minerals. In: Buccianti, A. et al. (Eds.), *Proceedings of the Arezzo Seminar on Fluids Geochemistry*. Paninieditore, Pisa, Italy, pp. 18–30.

Oelkers, E.H., Schott, J., 1995. Experimental study of anorthite dissolution rates and the relative mechanism of feldspar hydrolysis. *Geochim. Cosmochim. Acta* **59**, 5039–5053.

Oelkers, E.H., Schott, J., 1998. Does organic acid adsorption affect alkali-feldspar dissolution rates? *Chem. Geol.* **151**, 235–245.

Oelkers, E.H., Schott, J., 2001. An experimental study of enstatite dissolution rates as a function of pH, temperature, and aqueous Mg and Si concentration, and the mechanism of pyroxene/pyroxenoid dissolution. *Geochim. Cosmochim. Acta* **65**, 1219–1231.

Oelkers, E.H., Schott, J., Devidal, J.-L., 1994. The effect of aluminum, pH, and chemical affinity on the rates of aluminosilicate dissolution reactions. *Geochim. Cosmochim. Acta* **58**, 2011–2024.

Oelkers, E.H., Schott, J., Devidal, J.-L., 2001. On the interpretation of closed system mineral dissolution experiments. In: Huertas, R.J., Chou, L., Wollast, R. (Eds.), Comment on *Mechanism of kaolinite dissolution at room temperature and pressure. Part II. Kinetic Study. Geochim. Cosmochim. Acta* **65**, 4429–4432.

Oxburgh, R., Drever, J.L., Sun, Y.-T., 1994. Mechanism of plagioclase dissolution in acid solution at 25 °C. *Geochim. Cosmochim. Acta* **58**, 661–669.

Perret, D., Crovisier, J.L., Stille, P., Shields, G., Mäder, U., Advocat, T., Schenk, K., Chardonnens, M., 2003. Thermodynamic stability of waste glasses compared to leaching behaviour. *Appl. Geochem.* **18**, 1165–1184.

Plettinck, S., Chou, L., Wollast, R., 1994. Kinetics and mechanisms of dissolution of silica at room temperatures and pressure. *Min. Mag.* **58A**, 728–729.

Pokrovsky, O.S., Schott, J., 2000. Kinetics and mechanism of forsterite dissolution at 25 °C and pH from 1 to 12. *Geochim. Cosmochim. Acta* **64**, 3313–3325.

Ragnarsdottir, K.V., 1993. Dissolution kinetics of heulandite at pH 2–12 and 25 °C. *Geochim. Cosmochim. Acta* **57**, 2439–2449.

Rimstidt, J.D., Dove, P.M., 1986. Mineral/solution reaction rates in a mixed flow reactor: wollastonite hydrolysis. *Geochim. Cosmochim. Acta* **50**, 2509–2516.

Rosso, J.J., Rimstidt, D., 2000. A high resolution study of forsterite dissolution. *Geochim. Cosmochim. Acta* **64**, 797–811.

Schott, J., Berner, R.A., Sjöberg, E.L., 1981. Mechanism of pyroxene and amphibole weathering—I. Experimental studies of iron-free minerals. *Geochim. Cosmochim. Acta* **45**, 2123–2135.

Siegel, D.I., Pfannkuch, H.O., 1984. Silicate mineral dissolution at pH 4 and near standard temperature and pressure. *Geochim. Cosmochim. Acta* **48**, 197–201.

Spivack, A.J., Staudigel, H., 1994. Low-temperature alteration of the upper oceanic crust and the alkalinity budget of seawater. *Chem. Geol.* **115**, 239–247.

Stefánsson, A., Gíslason, S.R., 2001. Chemical weathering of basalts, SW Iceland. Effect of rock crystallinity and secondary minerals on chemical fluxes to the ocean. *Am. J. Sci.* **301**, 513–556.

Stillings, L.L., Brantley, S.L., 1995. Feldspar dissolution at 25 °C and pH 3. Reaction stoichiometry and the effect of cations. *Geochim. Cosmochim. Acta* **59**, 1483–1496.

Stillings, L.L., Drever, J.I., Brantley, S.L., Sun, Y.-T., Oxburgh, R., 1996. Rates of feldspar dissolution at pH 3–7 with 0–8 mM oxalic acid. *Chem. Geol.* **132**, 79–89.

Swoboda-Colberg, N.G., Drever, J.I., 1993. Mineral dissolution rates in plot-scale field and laboratory experiments. *Chem. Geol.* **105**, 51–69.

Taylor, A.S., Lasaga, A.C., 1999. The role of basalt weathering in the Sr isotope budget of the oceans. *Chem. Geol.* **161**, 199–214.

Taylor, A.S., Lasaga, A.C., Blum, J.D., 1999. Effect of lithology on silicate weathering rates. In: Ármannsson, H. (Ed.), *Geochemistry of the Earth's surface*. Balkema, Rotterdam, pp. 127–128.

van Hees, P.A.W., Lundström, U.S., Mörth, C.-M., 2002. Dissolution of microcline and labradorite in a forest O horizon extract: the effect of naturally occurring organic acids. *Chem. Geol.* **189**, 199–211.

Welch, S.A., Ullman, W.J., 1996. Feldspar dissolution in acidic and organic solutions. Compositional and pH dependence of dissolution rate. *Geochim. Cosmochim. Acta* **60**, 2939–2948.

White, A.F., 1983. Surface chemistry and dissolution kinetics of glassy rocks at 25 °C. *Geochim. Cosmochim. Acta* **47**, 805–815.

White, A.F., Brantley, S.L., 2003. The effect of time on the weathering of silicate minerals: why do weathering rates differ in the laboratory and field? *Chem. Geol.* **202**, 497–506.

Wieland, E., Stumm, W., 1992. Dissolution kinetics of kaolinite in acid aqueous solutions at 25 °C. *Geochim. Cosmochim. Acta* **56**, 3339–3355.

Weissbart, E.J., Rimstidt, J.D., 2000. Wollastonite: incongruent dissolution and leached layer formation. *Geochim. Cosmochim. Acta* **64**, 4007–4016.

Wogelius, R.A., Walther, J.V., 1991. Olivine dissolution at 25 °C: effects of pH, CO_2, and organic acids. *Geochim. Cosmochim. Acta* **55**, 943–954.

Wogelius, R.A., Walther, J.V., 1992. Olivine dissolution at near-surface conditions. *Chem. Geol.* **97**, 101–112.

Wolff-Boenisch, D., Gislason, S.R., Oelkers, E.H., Putnis, C.V., 2004a. The dissolution rates of natural glasses as a function of their

composition at pH 4 and 10.6, and temperatures from 25 to 74 °C. *Geochim. Cosmochim. Acta* **68**, 4843–4858.

Wolff-Boenisch, D., Gislason, S.R., Oelkers, E.H., 2004b. The effect of fluoride on the dissolution rates of natural glasses at pH 4 and 25 °C. *Geochim. Cosmochim. Acta* **68**, 4571–4582.

Zhang, H., Bloom, P.R., 1999. Dissolution kinetics of hornblende in organic acid solutions. *Soil Sci. Soc. Am. J.* **63**, 815–822.

Zhang, H., Bloom, P.R., Nater, E.A., Erich, M.S., 1996. Rates and stoichiometry of hornblende dissolution over 115 days of laboratory weathering at pH 3.6–4.0 and 25 °C in 0.01 M lithium acetate. *Geochim. Cosmochim. Acta* **60**, 941–950.

Zysett, M., Schindler, P.W., 1996. The proton promoted dissolution kinetics of K-montmorillonite. *Geochim. Cosmochim. Acta* **60**, 921–931.